



## Event by Event Studies of Au-Au Collisions at $\sqrt{s_{NN}} = 200 \text{ GeV}$ Using Two Event Generators

M.H.M. Soleiman\*

Physics Department, Faculty of Science, Cairo University Giza, Egypt

Received 20<sup>th</sup> Feb. 2019  
Accepted 14<sup>th</sup> Nov. 2019

The study of hadrons production in relativistic heavy ion collisions at STAR provides the researchers with valuable techniques to investigate the properties of quark gluon plasma (QGP) and the subsequent hadronizations. The present work aims at investigating the asymmetry in hadron and anti-hadron productions at the relativistic heavy ion collisions with parameters;  $\Delta\phi$ : the azimuthal angle of the transverse momentum vector  $\vec{p}_t$  with respect to the reaction plane,  $p_t$ : the transverse momentum,  $\eta$ : pseudo rapidity, and  $Y$ : the rapidity, and allowing for event by event (i.e. local) studies. *HIJING* and *HYDJET++* models were used to explain the data of the experiments produced at the *RHIC* for Au-Au relativistic collision by *STAR*, *PHENIX*, and *BRAHMS* experiments. Hadrons and the anti-hadrons productions are based on Monte Carlo techniques in the models. The particles selected for this study were proton and lambda ( $P^\pm, \Lambda^\pm$ ) for baryons, and pi and kaon ( $\pi^\pm, \kappa^\pm$ ) for mesons in order to determine the most probable production-asymmetries regions in phase-space of hadrons and anti-hadrons for heavy ions  $^{197}\text{Au}_{79} - ^{197}\text{Au}_{79}$  collisions at  $\sqrt{s_{NN}} = 200 \text{ GeV}$  with about  $\geq 800$  events, which are generated from each model event generator. It was found that *HYDJET++* 2.0.2 event generator is more realistic in comparing the results of simulations with those of the experimental data published by the *BRAHMS*, *PHENIX*, and *STAR* Collaboration.

**Keywords:** Heavy ion collision (HIC), RHIC, Proton and lambda, pi and kaon, Hadron and anti-hadron, Asymmetry sum ratio

### Introduction

Relativistic heavy-ion collisions create suitable conditions to study phase transitions from hadron to deconfined quark matter in the frame of Quantum Chromo-Dynamics (QCD) and to examine the lattice QCD calculations. The asymmetry in the production of hadrons and anti-hadrons reported in STAR (RHIC), ALICE (LHC) and ATLAS (LHC) experiments [1-3] is a motivation for detailed studies of the dependence of this asymmetry on the dynamical and geometrical parameters of the produced hadrons in relativistic heavy ion collisions.

As quantum wave-functions of the constituent nucleons are close enough, in momentum and coordinate space, they will overlap to produce a nucleus. The production rate for nuclei with baryon number  $B$  is proportional to the nucleon density in momentum and coordinate spaces raised to powers of  $B$ , and therefore exhibits exponential behaviour as a function of  $B$  [1]. In quark gluon plasma (QGP) and at vanishing baryon density, a well-defined transition exists, in which, color deconfinement starts and chiral symmetry is restored; the energy density increases by the latent heat of deconfinement, the critical temperature of the phase transition  $T_c$  is about  $175 \pm 10 \text{ MeV}$ . For temperatures  $> T_c$ , the state of matter is a plasma

of deconfined quarks and gluons, which can be probed by; Electromagnetic radiation, quarkonium spectra, Jet quenching, strange, charm, exotic hadrons, and heavy hadrons. QGP suffers successive phase transitions until they are clustered into unstable and colored hadrons, which, then, decay into stable or physical hadrons.

Many evidences have demonstrated that the quark gluon plasma (QGP) matter has been produced mainly in the central  $Au + Au$  collisions at RHIC energies [5]. In the collision process, large amounts of energy are deposited into a more extended volume than that achieved in elementary particle collisions. These nuclear interactions briefly produce hot and dense matter containing large numbers of quarks and less of antiquarks. Then, the QGP expands rapidly and cools down. QGP undergoes a transition into unstable hadron gas, producing hadrons, anti-hadrons, and even complete nuclei as was reported by RHIC-STAR experiment – USA in 2010 [6], where the discovery of anti-Helium 4 ( ${}^4\overline{\text{He}}$ ) shows the possibility of new approach of dynamics in producing anti-hadrons from QGP.

*HIJING* is an event generator for a model combining perturbative-QCD (pQCD) inspired models for multiple jet production with low- $p_T$  multistring phenomenology, A Monte Carlo event generator HIJING is developed to study jet and multi-particle production in high energy  $pp$ ,  $pA$ , and  $AA$  collisions. The model includes multiple minijet production, nuclear shadowing of parton distribution functions, and a schematic mechanism of jet interactions in dense matter. Glauber geometry for multiple collisions is used to calculate  $pA$  and  $AA$  collisions. The phenomenological parameters are adjusted to reproduce essential features of  $pp$  multiparticle production data for a wide energy range ( $\sqrt{s_{NN}} = 5 - 2000 \text{ GeV}$ ) [7, 8]. *HYDJET++2.0.2* event generator [9] includes detailed treatment of soft hadro-production as well as hard multi-parton production, and takes into account medium-induced parton re-scattering and energy loss. The main program *HYDJET++2.0.2* is written in the object-oriented C++ language under the ROOT environment [10].

The physics behind the production of the charge asymmetry in the distributions of hadron is exhibited with a discussion of the Kharzeev and Voloshin model of the self-induced magnetic field and the chiral charge separation [11, 12]. This

model is not included in either *HIJING 1.35* or *HYDJET++ 2.0.2* event generators, but the model is of a great interest in the understanding the physical phenomena associated with heavy ion collisions.

Our previous study [13] focused on the dynamical and geometrical parameters restricted in the reaction plane of each event. The present study is an extension of the previous study that sheds light on the whole space of dynamical and geometrical parameters within event by event formulation by defining the local asymmetry ratio sum ( $\zeta$ ).

The first section introduces the description of the geometrical and dynamical parameters, the definition of the local asymmetry ratio sum ( $\zeta$ ), and the physical conditions for generating events using *HIJING 1.35* and *HYDJET++ 2.0.2*. The next section presents the results of the simulation according to the models; *HIJING* and *HYDJET++*, and then the discussions including comparisons with related analysis on data from published literatures concerning collaborations from *STAR*, *PHENIX*, and *BRAHMS* experiments.

### Methods and concepts

The geometry of relativistic heavy ion collision of  ${}^{197}\text{Au}_{79} - {}^{197}\text{Au}_{79}$  was illustrated and discussed in a previous study [13]. The geometrical and dynamical parameters studied in this work will be defined and discussed in this section. The impact parameter ( $\vec{b}$ ) is the vector distance in Fermi (fm) between the centers of the two colliding nuclei. The collision is in the center of mass (c.m.) frame of reference and along the z-axis. The plane containing z-axis and  $\vec{b}$  is the reaction plane ( $R.P.$ ), while the transverse plane is the xy-plane. The angle of  $\vec{b}$  with the x-axis is known as the reaction plane angle ( $\psi$ ). The projection of the momentum of any outcome-particle on the transverse plane is the transverse momentum ( $P_T$ ), while the projection onto the reaction plane is the in-reaction plane transverse momentum ( $P_{T_{in}}$ ). The angle between the transverse momentum  $P_T$  and the impact parameter vector  $\vec{b}$  is ( $\Delta\phi = \phi - \psi$ ), where  $\phi$  is the azimuthal angle of the particle momentum. The polar angle ( $\theta$ ) is the angle between the outgoing particle momentum and the z-axis, it is vital in calculation of the pseudo-rapidity ( $\eta$ ) and the rapidity ( $y$ ) [14],

$$y = \text{arctanh}(p/E) = 1/2 \ln|(E + P)/(E - P)|. \quad (1)$$

Where,  $E$  and  $p$  are the particle's total energy and the magnitude of its momentum respectively. The experimentalists prefer to define the rapidity ( $y$ ) as:

$$y = \operatorname{arctanh}(p_z/E) = 1/2 \ln|(E + P_z)/(E - P_z)|. \quad (2)$$

Where it is more symmetric at  $y = 0$ . In this work, the definition in equation (2) is used. The pseudo rapidity is suitable at the limit of zero mass (ultra-relativistic limit).

$$\eta = -\ln(\tan(\theta/2)), \quad (3)$$

The centrality measures, the amount of the nucleons from the two colliding nuclei participating in the formation of QGP, and is calculated as found in an earlier publication [15]:

$$cent = 1 - N_{part}/N_{total}, \quad (4)$$

$$N_{part} = N_{p\ part} + N_{T\ part},$$

$$N_{total} = A_{projectile} + A_{target} = 2 \times 197. \quad (5)$$

Where  $N_{total}$  is the total number of the nucleons included in the colliding nuclei, and  $N_{part}$  is the number of the participant nucleons in the formation of QGP, and equals to the sum of the participants nucleons from the projectile and from the target nuclei  $N_{p\ part}$  and  $N_{T\ part}$  respectively.

In the present study, a parameter ( $\zeta$ ) is defined to quantify the event by event asymmetry (we use the name 'local asymmetry parameter' in opposite to the global studies, which merge all events in one big event and defines global ratios). The local asymmetry ratio sum ( $\zeta$ ) is defined as:

$$\zeta = \frac{\sum_{events} \frac{N_{(Anti\ particle)} - N_{particles}}{N_{(Anti\ particle)} + N_{particles}}}{N_{events} \leq \zeta \leq N_{events}}. \quad (6)$$

The anti-hadron to hadron ratios (ah/h) are usually used in literatures and used in this work for the comparison with the published analysis of the experimental data from BRAHMS, PHENIX, STAR [16, 17, 18].

Two common event generators HIJING 1.35 and HYDJET++ 2.0.2 are used to generate samples of events under the following conditions:

- 1- The collision is between two heavy ions  $AA$  where  $A = {}^{197}\text{Au}_{79}$ .
- 2-  $\sqrt{s_{NN}} = 200 \text{ GeV}$ .

- 3- The PYTHIA 8.0 is included to model the nucleon-nucleon collisions.
- 4- The hadronization procedures are allowed without final hadron decays.
- 5- The impact parameter is determined by the minimum bias Gaussian distribution.
- 6- The experimental cuts are taken into account throughout the analysis, only if required for the comparison with the published data.
- 7- The number of generated events is 800 events on HIJING 1.35, and 1000 events on HYDJET++ 2.0.2.

### Results and Discussions

In this study, the geometrical parameters (the azimuthal angle  $\Delta\phi = \phi - \psi$ , and the pseudorapidity  $\eta = -\ln(\tan(\theta/2))$  where  $\theta$  is the polar angle with respect to the incidence axis) are studied from the point of view of the ah/h ratios for the comparison with the published analysis of the experimental data and the local asymmetry ratio sum  $\zeta$  for each of the studied hadrons ( $\pi^\pm, \kappa^\pm, p^\pm, \Lambda^\pm$ ).

Figures (1 and 2) present the local analysis of the asymmetry ratio sum  $\zeta$  over  $\Delta\phi$ . The results for HIJING 1.35 are presented in Fig. (1). The mean number of the produced  $\bar{\pi}$  is the same as that for  $\pi$  mesons over all azimuthal angles  $0 \leq \Delta\phi \leq 2\pi$ . The asymmetry sum ratio  $\zeta$  is stable for  $\kappa^\pm, p^\pm$ , and all heavy baryons that are greater than heavy hadrons of masses  $\geq$  the mass of  $\Lambda^\pm$  (ambiguity in mass spectrum for heavy hadrons on HIJING 1.35 was previously mentioned [13]). The other studied hadrons showed that the production of hadron is more than the anti-hadron which is prominent for protons. Figure (2) reveals the results of HYDJET++ 2.0.2. The mesons behave similarly as in Figure (1), but the baryons show preferred azimuthal directions for the emission of anti-baryons. The preferred emission angles  $\Delta\phi$  for baryons ( $p^\pm, \Lambda^\pm$ ) are  $\Delta\phi = 2.3$  and  $5.4 \text{ rad}$ . The asymmetry ratio sum  $\zeta$  is statistically a stable parameter for measuring the asymmetry in distributions of hadrons and anti-hadrons. Voloshin and Kharzeev effects of self-induced magnetic fields and the separation of partons and anti-partons are not included in either of the two event generators. The local asymmetry appears for baryons in Fig. (2) of HYDJET++ 2.0.2 is attributed to mechanical effects throughout interactions, such as the interaction between the

induced collective angular momentum and the directional flows in the participants of the heavy ion collisions.

The published data about  $\Delta\phi$  parameter are the correlations between the elliptic flow parameter  $v_2$  and the transverse momentum  $p_T$ . The equation used in the calculation of the elliptic flow parameter  $v_2$  was formulated earlier [18]:

$$dN/d\Delta\phi = A[1 + 2v_2 \cos 2\Delta\phi], \quad (7)$$

Where  $A$  and  $v_2$  are the fitting parameters,  $N$  is the yield of a specific hadron as a function of  $\Delta\phi$ . Fig. (3,4) and 5) present the comparisons of the available published experimental data for  $v_2(ah)/v_2(h)$  ratios [18] with the corresponding analysis on the events generated using HYDJET++ 2.0.2 for the hadrons  $\pi^\pm$  (The curve is scaled by a factor  $(12.5)^{-1}$ ),  $p^\pm$  (The curve is scaled by a factor  $(14)^{-1}$ ), and  $\Lambda^\pm$  (The curve is scaled by a factor  $(20.28)^{-1}$ ), respectively.

The analysis on the events generated by HIJING1.35 are excluded from this Figures because of the inconsistency between the conditions of the analysis and the cuts on the data, especially for  $\Lambda^\pm$ . HYDJET++ 2.0.2 which is consistent with the data as follows: in the range  $1 \leq p_T \leq 1.4 \text{ GeV}/c$  for  $\pi^\pm$ ,  $p_T \leq 1.1 \text{ GeV}/c$  for  $p^\pm$ , and  $p_T \leq 1.3 \text{ GeV}/c$  for  $\Lambda^\pm$ . Outside these ranges, there is no available data and the behavior of HYDJET++ 2.0.2 is spurious, namely, it either increases or decreases in an unexpected physical behavior. Fig. (6) shows the HYDJET++ 2.0.2 behavior on  $v_2(ah)/v_2(h)$  with  $p_T$  correlations for  $\kappa^\pm$ . The curve shows a peak at  $p_T = 1.26 \text{ GeV}/c$ , which is a signature for asymmetry of the elliptical flow in the transverse plane. HYDJET++ 2.0.2 shows a realistic behavior with the experimental data.

Charged hadrons distributions over the polar angle  $\theta$  in the center of the mass system is a good prop for the properties of QGP. The polar angle  $\theta$  has a range from 0 to  $\pi$ . Experimental setups are designed to measure of pseudo rapidity  $\eta$ . Pseudo rapidity density  $(\frac{dN_{ch}}{d\eta} \frac{1}{N_{ch}})$  distributions of the charged hadrons  $N_{ch}$  over  $\eta$  is vital in measuring mid-rapidity value [21].

Fig. (7) for HIJING 1.35 and Fig. (8) for HYDJET++ 2.0.2 present the local analysis in the asymmetry ratio sum  $\zeta$  for the pseudo rapidity  $\eta$ . The asymmetry ratio sum  $\zeta$  shows a stable and

symmetric behavior over the range  $-4 \leq \eta \leq 4$  for all studied hadrons produced in events generated by HIJING 1.35 as shown in Fig. (7). While the number of anti-mesons is similar to the number of mesons in the range  $4 \leq |\eta| \leq 6$ . The baryon production exceeds the anti-baryon production by about the ratio  $\frac{480}{800}$  for protons and  $\frac{300}{800}$  for heavy hadrons, where 800 is the number of generated events on HIJING 1.35. These effects are coming out due to the kinematic behavior of QGP ellipsoid, the asymmetry in collective flows, and the hadronization model of string-Lund hadronization model are included in HIJING 1.35. The asymmetry ratio sum  $\zeta$  shows an unstable and asymmetric behavior over the range  $-4 \leq \eta \leq 4$  for three of the studied hadrons ( $\kappa^\pm, p^\pm, \Lambda^\pm$ ) produced in events generated by HYDJET++ 2.0.2 as shown in Fig. (8). The range of  $4 \leq |\eta| \leq 6$  shows a stability and symmetry for all hadrons produced in events generated by HYDJET++ 2.0.2. The calculated curves of  $\zeta$  in Fig. (8) of the model HYDJET++ 2.0.2 are the inversions of the calculated curves in Fig. (7) of the model HIJING 1.35. In Fig. (8), the range of  $-4 \leq \eta \leq 4$  has been characterized by the following: the produced kaons exceeds the anti-kaons by the mean ratio  $\frac{30}{1000}$ , the produced lambda exceeds the anti-lambda by the mean ratio  $\frac{100}{1000}$ , and the produced proton exceeds anti-proton by the ratio  $\frac{163}{1000}$ , where 1000 is the number of generated events on HYDJET++ 2.0.2. The inversion effect is due to directional flow and the multi-parton interaction processes allowed in HYDJET++ 2.0.2. The asymmetry of anti-hadron production over  $\eta$  is due to the directional flow and the hadronization algorithms used in HYDJET++ 2.0.2.

kinematic behavior of QGP ellipsoid of the participants in the model HYDJET++ are coming from the assumptions of the elliptic shape of the initial QGP with the major axis of the ellipsoid along the perpendicular to the reaction-plane and the generation of the anti-quarks near the ellipsoid major axis, the hadrons must be dominant at  $\theta \simeq 0, \pi$  (i. e. at large  $\eta$ ) and anti-hadrons production must rise at the poles of the ellipsoid  $\theta \simeq \frac{\pi}{2}$  (i. e. at  $\eta \simeq 0$ ). The asymmetry in the distributions of the charged hadrons could be observed very effectively using the statistically stable parameter of the asymmetry ratio sum  $\zeta$ .

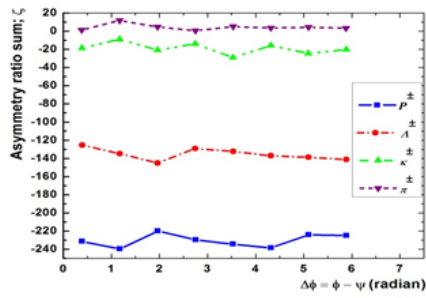


Fig. (1): ah/h event asymmetry ratio sum  $\zeta$  with respect to azimuthal angle  $\Delta\phi$  using HIJING 1.35 simulator

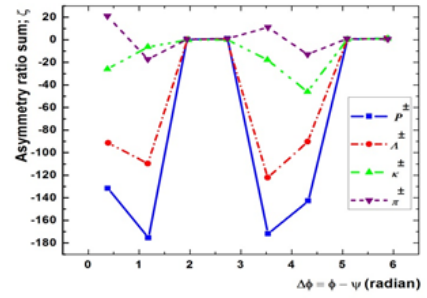


Fig. (2): ah/h event asymmetry ratio sum  $\zeta$  with respect to azimuthal angle  $\Delta\phi$  using HYDJET++ 2.0.2 simulator

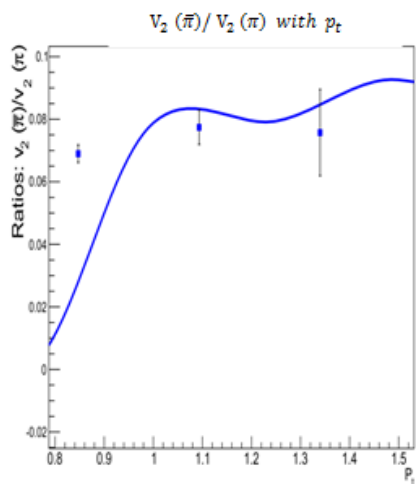


Fig. (3): The comparison of the available published experimental data [18] for  $v_2(ah)/v_2(h)$  ratios with the corresponding analysis on the events generated using HYDJET++ 2.0.2 for pi-meson  $\pi^\pm$

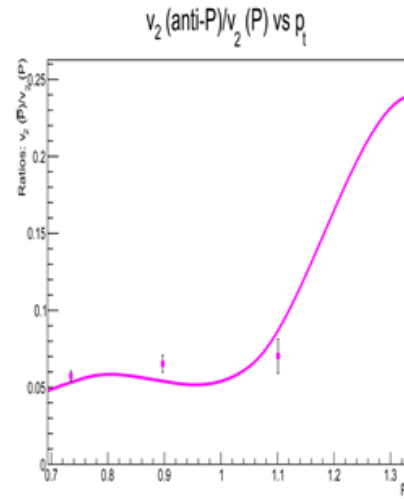


Fig. (4): The comparison of the available published experimental data [18] for  $v_2(ah)/v_2(h)$  ratios with the corresponding analysis on the events generated using HYDJET++ 2.0.2

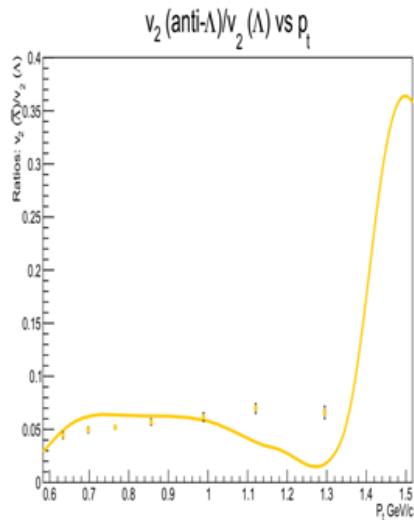


Fig. (5): The comparison of the available published experimental data [18] for  $v_2(ah)/v_2(h)$  ratios with the corresponding analysis on the events generated using HYDJET++ 2.0.2 for Lambda baryon  $\Lambda^\pm$

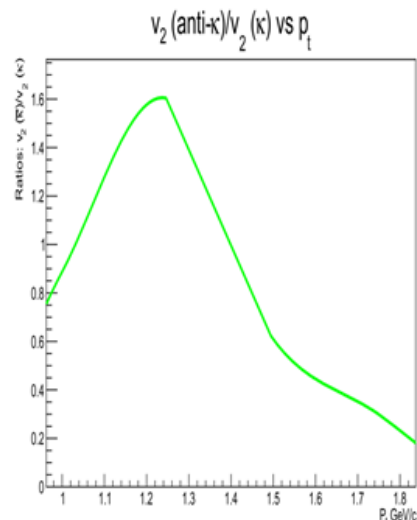


Fig. (6): The HYDJET++ 2.0.2 behaviour on  $v_2(ah)/v_2(h)$  with  $p_T$  correlations for Kaon-meson  $\kappa^\pm$

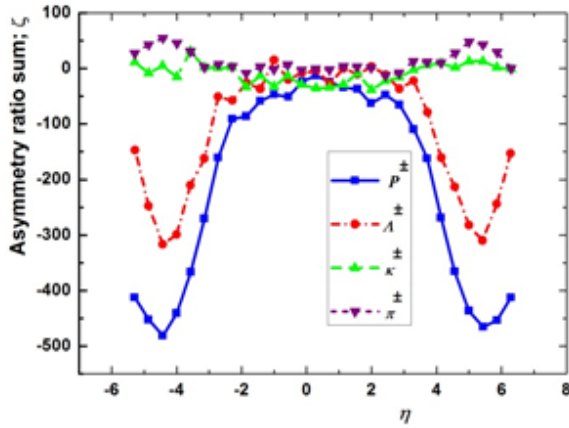


Fig. (7): ah/h event asymmetry ratio sum with respect to pseudorapidity  $\eta$  using HIJING 1.35 simulator

A previous study [19] revealed the asymmetry in the emission of the charged particles by the correlation and the small angle correlation methods and showed that the tendency in  $d + Au$  and peripheral  $Au + Au$  collisions of back-to-back emission of same-sign particles is weaker in the out-of-reaction-plane than in the in-reaction-plane directions, and the particles within one unit of pseudo rapidity are preferentially emitted in the same direction irrespective, they are of the same or opposite charge signs. On the other hand, for the medium-central to central collisions, the opposite-sign pairs are still preferentially aligned in the same direction and more than in peripheral collisions. The same sign pairs are preferentially back-to-back. Thus, the small-angle correlation between the opposite-sign pairs is always stronger out-of-reaction-plane compared to the in-reaction-plane. The results obtained from Figures (7 and 8) are in agreement with those obtained in a earlier publication [19]. The rapidity  $y$  was defined to measure the boost of the relativistic hadrons emitted from the QGP on a logarithmic scale. It is expected that the rapidity  $y$  must be dynamically and geometrically symmetric. Figures (9 and 10) illustrate the local analysis using the asymmetry ratio sum  $\zeta$  for rapidity  $Y$ . Fig. (9) shows the results for HIJING 1.35, where the rapidity for  $\pi^\pm, \kappa^\pm$  are stable and symmetric around  $y = 0$  and less symmetric for  $p^\pm$  and heavy hadrons with large variations over the range of  $y$  ( $-6.4 \leq y \leq 6.4$ ). HIJING 1.35 predicts that the number of hadrons is equal to the number of anti-hadrons around  $y = 0$ , and the baryons are dominated over the anti-baryons ( $p^\pm, \Lambda^\pm$ ) at ( $y \approx \pm 5.2$ ). Fig. (10)

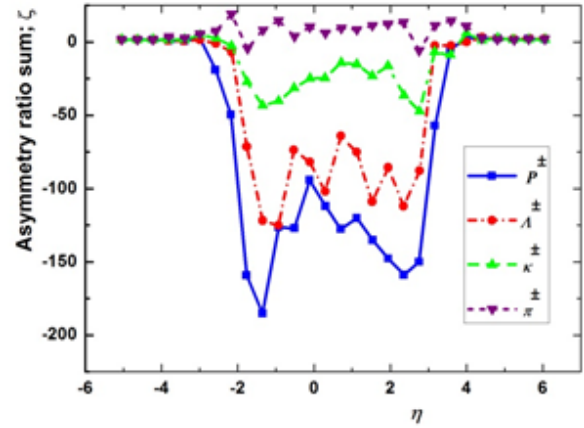


Fig. (8): ah/h event asymmetry ratio sum with respect to pseudorapidity  $\eta$  using HYDJET++ 2.0.2 simulator

presents the same local analysis conducted for events generated by HIJING 2.2. The rapidity for  $\pi^\pm, \kappa^\pm$  are stable and symmetric around  $y = 0$  and less symmetric for  $p^\pm$  and  $\Lambda^\pm$  with high stability at values of  $\zeta_p \approx -150, \zeta_\Lambda \approx -100$ . HYDJET++ 2.0.2 predicts that over all the rapidity range, the baryons dominate the anti-baryons, but the mesons and anti-mesons are balanced in production.

Figures (11 – 16) show the comparison of the ah/h ratios for rapidity  $y$  with the published experimental data [16] with the following cuts 1- centrality (0% to 20%), 2-  $p_T \geq 0.5 \text{ GeV}/c$ , 3-  $|y| \leq 3$ . The published experimental data are found to be available for  $\pi^\pm, \kappa^\pm, p^\pm$ . The results from HIJING1.35 are deviated largely away from the experimental data after  $|y| \leq 2$ , but the results for HYDJET++ 2.0.2 are in a good coincidence with the experimental data except for  $p^\pm, \kappa^\pm$ . HYDJET++ 2.0.2 is more realistic than HIJING 1.35 compared to the data for rapidity  $y$ . Figures (17) and (18) show the asymmetry ratio sum  $\zeta$  for  $p_T$ . It has been observed that the behaviour of the four curves of studied particles, ( $\pi^\pm, \kappa^\pm, p^\pm, \Lambda^\pm$ ), are similar and the defect in HIJING 1.35 has no effects. The Figures (from 19 to 31) show the comparison of the experimental data with the corresponding analysis at different centralities (from 0% to 5% in Figures (19 to 25), and from 60% to 92% in Figures (26 to 31)) on the events generated using HIJING 1.35 and HYDJET++ 2.0.2. HYDJET++ 2.0.2 shows a realistic behavior with experimental data in the transverse momentum  $p_t$ , especially for ( $\pi^\pm, \kappa^\pm, p^\pm$ ).

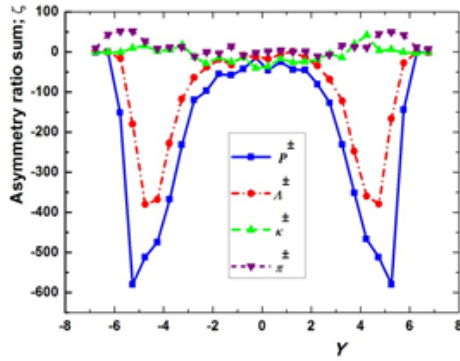


Fig. (9): ah/h event asymmetry ratio sum with respect to rapidity y using HIJING 1.35 simulator

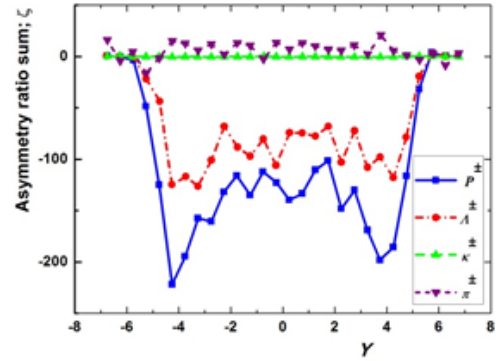


Fig. (10): ah/h event asymmetry ratio sum with respect to rapidity y using HYDJET++ 2.0.2 simulator

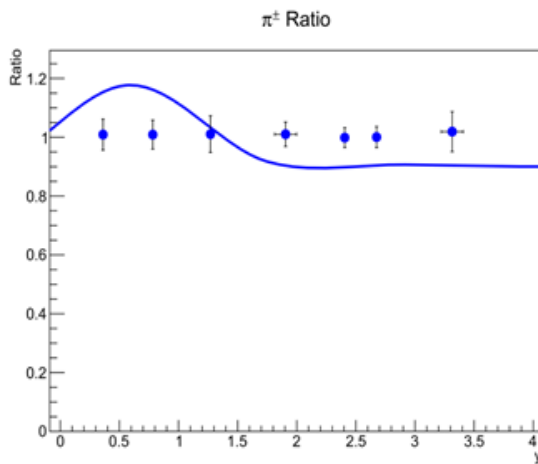


Fig. (11): The y dependence of ah/h ratio for  $\pi^\pm$  meson (with centrality 0% to 20%). The solid line represents the results from the global analysis of the events generated by HIJING 1.35. The points with error bars are the experimental published data [16]

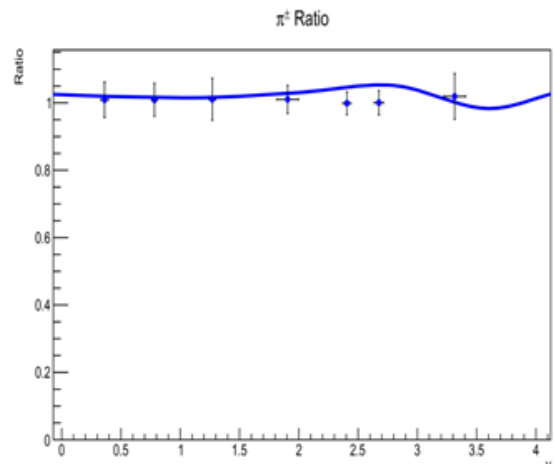


Fig. (12): The y dependence of ah/h ratio for  $\pi^\pm$  meson (with centrality 0% to 20%). The solid line represents the results from the global analysis of the events generated by HYDJET++2.0.2. The points with error bars are the experimental published data [16]

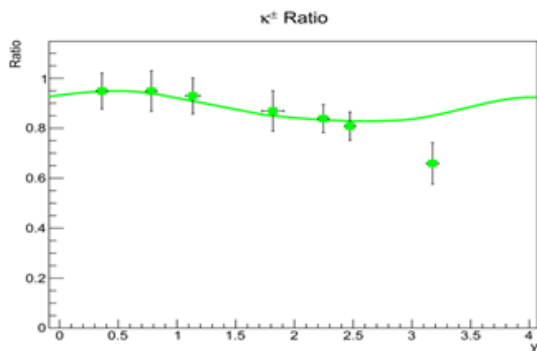


Fig. (13): The y dependence of ah/h ratio for  $\kappa^\pm$  meson (with centrality 0% to 20%). The solid line represents the results from the global analysis of the events generated by HIJING 1.35. The points with error bars are the experimental published data [16]

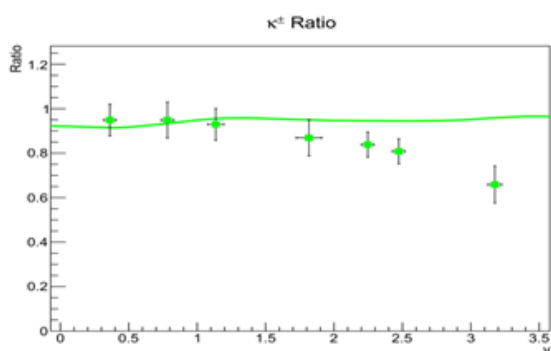


Fig. (14): The y dependence of ah/h ratio for  $\kappa^\pm$  meson (with centrality 0% to 20%). The solid line represents the results from the global analysis of the events generated by HYDJET++2.0.2. The points with error bars are the experimental published data [16]

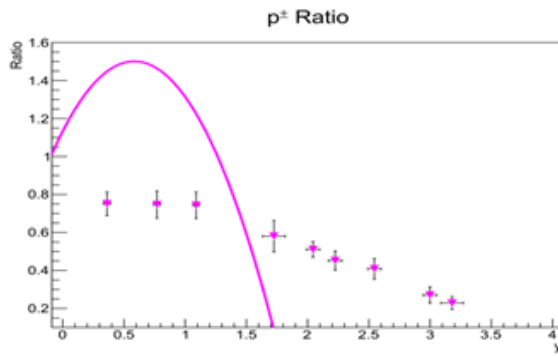


Fig. (15): The y dependence of ah/h ratio for  $p^\pm$  (with centrality 0% to 20%). The solid line represents the results from the global analysis of the events generated by HIJING 1.35. The points with error bars are the experimental published data [16]

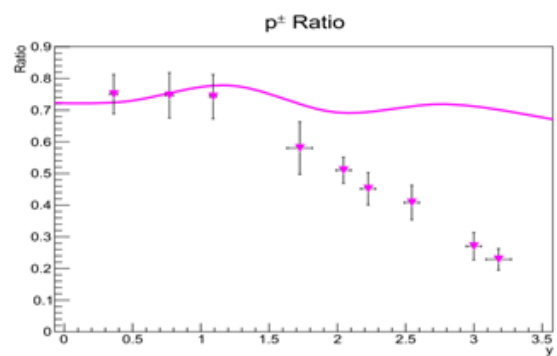


Fig. (16): The y dependence of ah/h ratio for  $p^\pm$  (with centrality 0% to 20%). The solid line represents the results from the global analysis of the events generated by HYDJET++ 2.0.2. The points with error bars are the experimental published data [16]

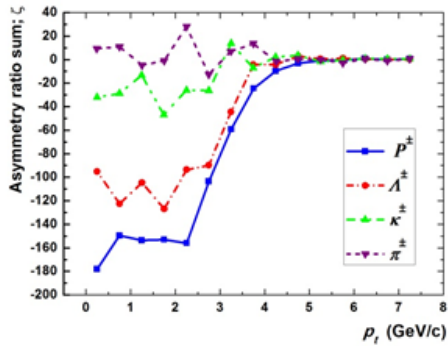


Fig. (17): ah/h event asymmetry ratio sum with respect to transverse momentum  $p_T$  using HIJING 1.35 simulator

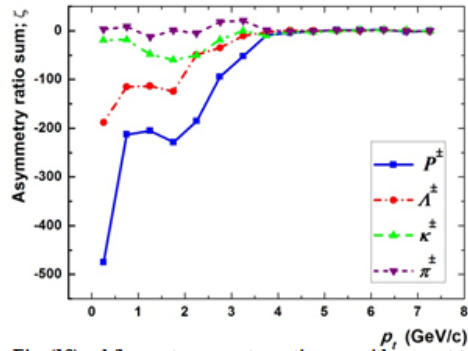


Fig. (18): ah/h event asymmetry ratio sum with respect to transverse momentum  $p_T$  using HYDJET++ 2.0.2 simulator

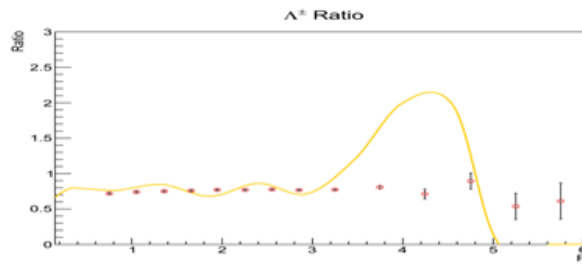


Fig. (19): The  $p_T$  dependence of ah/h ratio for  $\Lambda^\pm$  (with centrality 0% to 10%). The solid line represents the results from the global analysis of the events generated by HYDJET++ 2.0.2. The points with error bars are the experimental published data [22]

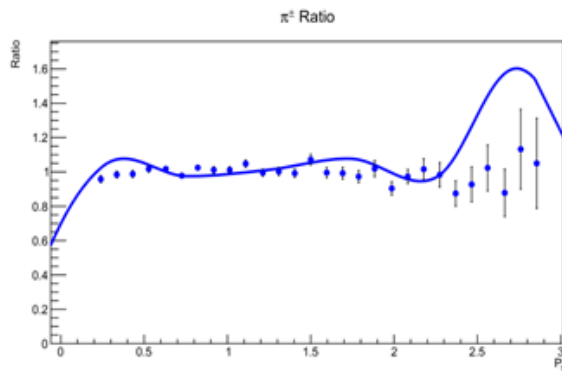


Fig. (20): The  $p_T$  dependence of ah/h ratio for  $\pi^\pm$  meson (with centrality 0% to 5%). The solid line represents the results from the global analysis of the events generated by HIJING 1.35. The points with error bars are the experimental published data [17]

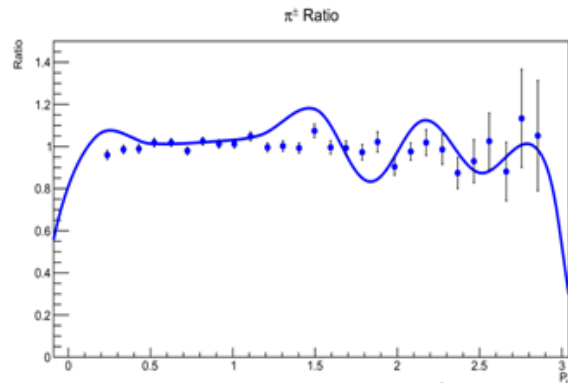


Fig. (21): The  $p_T$  dependence of ah/h ratio for  $\pi^\pm$  meson (with centrality 0% to 5%). The solid line represents the results from the global analysis of the events generated by HYDJET++2.0.2. The points with error bars are the experimental published data [17]

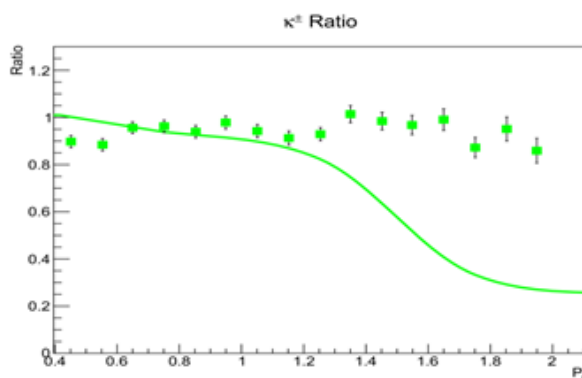


Fig. (22): The  $p_T$  dependence of ah/h ratio for  $\kappa^\pm$  meson (with centrality 0% to 5%). The solid line represents the results from the global analysis of the events generated by HIJING 1.35. The points with error bars are the experimental published data [17]

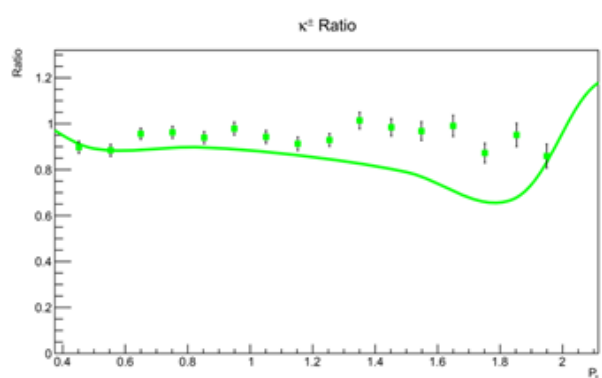


Fig. (23): The  $p_T$  dependence of ah/h ratio for  $\kappa^\pm$  meson (with centrality 0% to 5%). The solid line represents the results from the global analysis of the events generated by HYDJET++2.0.2. The points with error bars are the experimental published data [17]

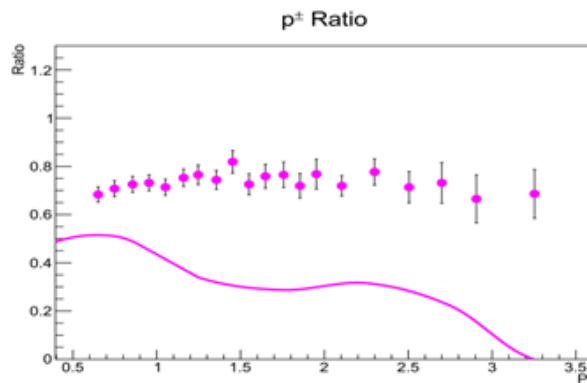


Fig. (24): The  $p_T$  dependence of ah/h ratio for  $p^\pm$  (with centrality 0% to 5%). The solid line represents the results from the global analysis of the events generated by HIJING 1.35. The points with error bars are the experimental published data [17]

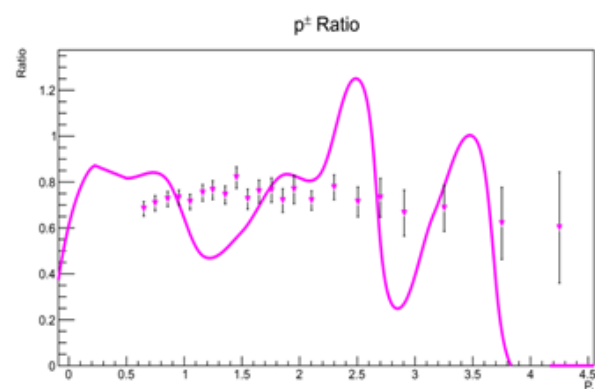


Fig. (25): The  $p_T$  dependence of ah/h ratio for  $p^\pm$  (with centrality 0% to 5%). The solid line represents the results from the global analysis of the events generated by HYDJET++2.0.2. The points with error bars are the experimental published data [17]

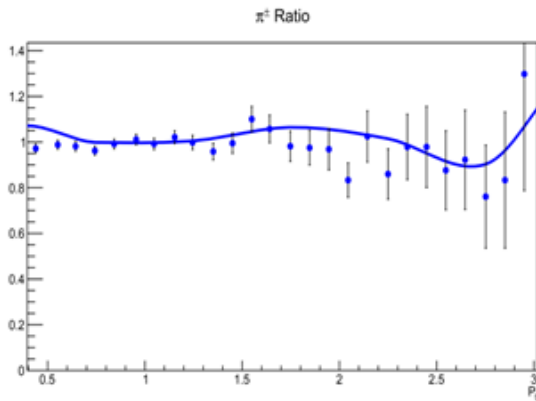


Fig. (26): The  $p_T$  dependence of  $ah/h$  ratio for  $\pi^\pm$  meson (with centrality 60% to 92%). The solid line represents the results from the global analysis of the events generated by HIJING 1.35. The points with error bars are the experimental published data [17]

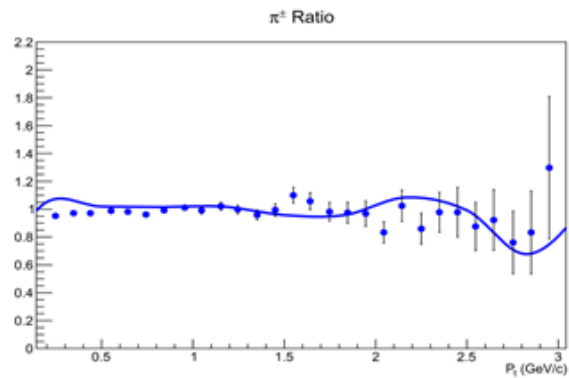


Fig. (27): The  $p_T$  dependence of  $ah/h$  ratio for  $\pi^\pm$  meson (with centrality 60% to 92%). The solid line represents the results from the global analysis of the events generated by HYDJET++2.0.2. The points with error bars are the experimental published data [17]

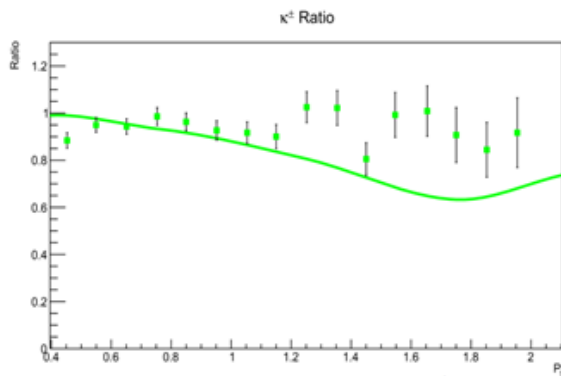


Fig. (28): The  $p_T$  dependence of  $ah/h$  ratio for  $\kappa^\pm$  meson (with centrality 60% to 92%). The solid line represents the results from the global analysis of the events generated by HIJING 1.35. The points with error bars are the experimental published data [17]

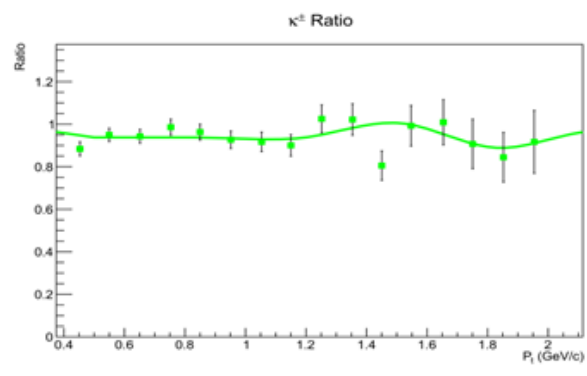


Fig. (29): The  $p_T$  dependence of  $ah/h$  ratio for  $\kappa^\pm$  meson (with centrality 60% to 92%). The solid line represents the results from the global analysis of the events generated by HYDJET++2.0.2. The points with error bars are the experimental published data [17]

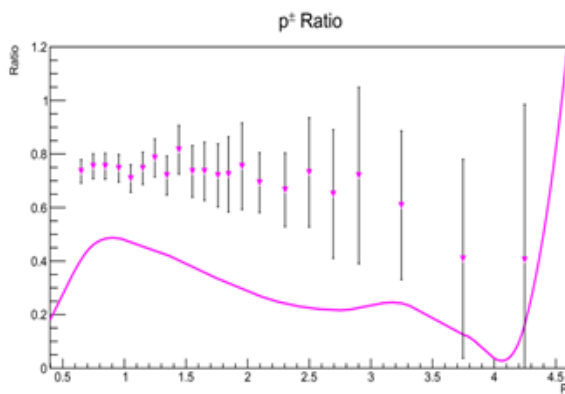


Fig. (30): The  $p_T$  dependence of  $ah/h$  ratio for  $p^\pm$  (with centrality 60% to 92%) The solid line represents the results from the global analysis of the events generated by HIJING 1.35. The points with error bars are the experimental published data [17]

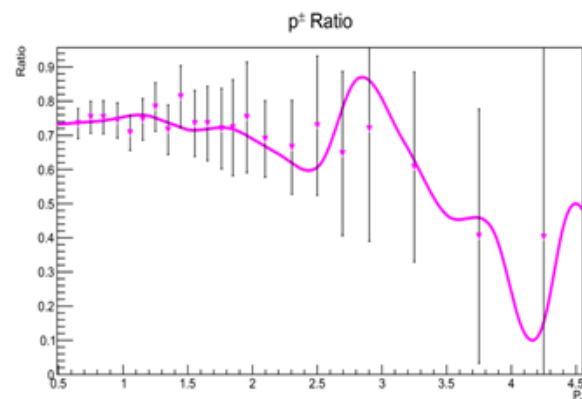


Fig. (31): The  $p_T$  dependence of  $ah/h$  ratio for  $p^\pm$  (with centrality 60% to 92%). The solid line represents the results from the global analysis of the events generated by HYDJET++2.0.2. The points with error bars are the experimental published data [17]

### Conclusions

The current work presents a comparative study of the charge asymmetry distributions over dynamical and geometrical parameters for two mesons  $\pi^\pm, \kappa^\pm$  and two baryons  $p^\pm, \Lambda^\pm$  produced in the events generated by each of the event generators HIJING 1.35 and HYDJET++ 2.0.2 at  $\sqrt{s_{NN}} = 200 \text{ GeV}$  in the center of mass system. The number of the generated events is 800 events on HIJING 1.35, and 1000 events on HYDJET++ 2.0.2. The conditions of the generated events are; the hadronization procedures are allowed without final hadron decays, the impact parameter is determined by the minimum bias Gaussian distribution, and the experimental cuts are taken into account throughout the analysis. Local analysis, where the asymmetry parameters are evaluated for each event using the asymmetry ratio sum  $\xi$ , is proposed. The physics included in each of the models; HIJING and HYDJET++ are considered in the interpretation of the analysis-results and in driving the conclusions. The ROOT 5.34 environment for the data analysis, graphing, and mathematical algorithms is used in calculations and in producing the graphs.

- 1- HIJING 1.35 predicts that; the number of hadrons is equal to the number of anti-hadrons around rapidity  $y = 0$ , and the baryons are dominated over the anti-baryons ( $p^\pm, \Lambda^\pm$ ) at ( $y \approx \pm 5.2$ ). HYDJET++ 2.0.2 predicts that over all the rapidity range the baryons dominates the anti-baryons, but the mesons and anti-mesons are balanced in production. HIJING1.35 are deviated largely away from the experimental data where  $|y| \leq 2$ , but the results for HYDJET++ 2.0.2 are in a good coincidence with the experimental data except for  $p^\pm, \kappa^\pm$ .
- 2- The asymmetry ratio sum  $\zeta$  shows a stable and symmetric behaviour over the range  $-4 \leq \eta \leq 4$  for all studied hadrons produced in events generated by HIJING 1.35, while the number of anti-mesons is similar to the number of mesons in the range  $4 \leq |\eta| \leq 6$ , the baryon production exceeds the anti-baryon production by about the ratio  $\frac{480}{800}$  for protons and  $\frac{300}{800}$  for heavy hadrons, where 800 is the number of generated events on HIJING 1.35. The asymmetry ratio sum  $\zeta$  show an unstable and asymmetric behaviour over the range  $-4 \leq$

$\eta \leq 4$  for three of the studied hadrons  $\kappa^\pm, p^\pm, \Lambda^\pm$  produced in events generated by HYDJET++ 2.0.2. The range of  $4 \leq |\eta| \leq 6$  shows a stability and symmetry for all hadrons produced in events generated by HYDJET++ 2.0.2. The calculated curves of  $\zeta$  in HYDJET++ 2.0.2 are the inversion of the calculated curves in HIJING 1.35. In the range of  $-4 \leq \eta \leq 4$ , the produced kaons exceeds the anti-kaons by the mean ratio  $\frac{30}{1000}$ , the produced lambda exceeds the anti-lambda by the mean ratio  $\frac{100}{1000}$ , and the produced proton exceeds anti-proton by the ratio  $\frac{163}{1000}$ , where 1000 is the number of generated events on HYDJET++ 2.0.2.

- 3- The asymmetry of anti-hadron production over  $\eta$  is due to the directional flow and the hadronization algorithms used in HYDJET++ 2.0.2.
- 4- The asymmetry in the production of hadron and anti-hadron could be observable throughout the analysis using the asymmetry ratio sum  $\zeta$ . The asymmetry ratio sum  $\zeta$  is statistically stable quantity and effective in the analysis of the anti-hadron production asymmetry.
- 5- As HYDJET++ 2.0.2 has been shown to be more realistic than HIJIN 1.35 in the study of dynamical parameters, It could be considered that the behaviour of the asymmetry ratio sum  $\zeta$  is a good representation of what be gotten from the experimental measurements. The asymmetry in the distributions of charged hadrons could be observed very effectively using the statistically stable parameter of the asymmetry ratio sum  $\zeta$ .

Finally, HYDJET++ 2.0.2 uses a more stable hadronization models. HYDJET++ 2.0.2 is more realistic model than HIJING 1.35 from the point of view of the comparison with available published experimental data [16-19, 22].

### ACKNOWLEDGEMENT

The author is grateful to Professor Dr. Sayed Saleh Abdel-AZIZ, Physics Department, Cairo University, for his helpful advice and discussion throughout the result production and the paper writing.

**References**

1. STAR collaboration, Science 328, VOL58, (2010).
2. ALICE Collaboration, R. Belmont, Nuclear Physics A 931, (2014), 981–985.
3. ATLAS Collaboration, G. Aad et al., JHEP05, (2015), 061.
4. Helmut Satz, Nuclear Physics A, 862–863, (2011), 4–12.
5. STAR Collaboration, J. Adams et al., Nucl. Phys. A, (2005), 757- 102.
6. STAR Collaboration, B. I. Abelev et al., Nature, (2011), 473- 353.
7. I. Zh. Bunzarov, N. Y. Chankova\_Bunzarova and O. V. Rogachevsky, ISSN 1547\_4771, Physics of Particles and Nuclei Letters, Vol. 11, No. 4, (2014), pp. 404–409.
8. Fermilab E557 Collaboration, C. Stewart et al., Phys. Rev. D 42, (1990), 1385.
9. I.P. Lokhtin, L.V. Malinina, S.V. Petrushanko, A.M. Snigirev, I. Arsene and K. Tywoniuk, Compu Phys. Commun., Volume 180, Issue 5, May (2009), Pages 779–799.
10. R. Brun and F. Rademakers, Nucl. Instrum. Meth., A 389 (1997) 81; (<http://root.cern.ch>).
11. D.E. Kharzeev et al., Nuclear Physics A 803 (2008), 227–253.
12. S. A. Voloshin and A. M. Poskanzer, Phys. Lett. B 474, (2000), 27-32.
13. M.H.M. Soleiman, S.S. Abdel-Aziz, and M.S.E. Sobhi, ISVHECRI 2016, EPJ Web of Conferences 145, (2017), 19017.
14. Ramona Vogt, “ultrarelativistic heavy-ion collisions”, Elsevier B.V., (2007).
15. Raimond Snellings, New J. Phys. 13, (2011), 055008.
16. BRAHMS Collaboration, I. G. Bearden et al., Phys. Rev. Lett. 90, (2003), 102301.
17. PHENIX Collaboration, S. S. Adler et al., Phys. Rev. C 69, (2004), 034909.
18. STAR Collaboration, J. Adams et al., Phys. Rev. Lett. 95, (2005), 12230.
19. STAR Collaboration, L. Adamczyk et al., Phys. Rev. C 89, (2014), 044908.
20. STAR Collaboration, B. I. Abelev et al., Phys. Rev. Lett. 103, (2009), 251601.
21. ALICE Collaboration, B. Abelev et al., arXiv:1210.3615v2 [nucl-ex], 25 Feb (2013).
22. STAR Collaboration, M. A. C. Lamont, J. Phys. G: Nucl. Part. Phys. 30, (2004), S963–S967.